INTERFACE

royalsocietypublishing.org/journal/rsif

Research

Cite this article: Yu Q, Kolomeisky AB, Igoshin OA. 2022 The energy cost and optimal design of networks for biological discrimination. *J. R. Soc. Interface* **19**: 20210883.
https://doi.org/10.1098/rsif.2021.0883

Received: 23 November 2021
Accepted: 2 February 2022

Subject Category:
Life Sciences–Physics interface

Subject Areas:
bioenergetics, biophysics, systems biology

Keywords:
kinetic proofreading, energy dissipation, cellular energetics, non-equilibrium thermodynamics, biochemical networks, reaction kinetics and dynamics

Author for correspondence:
Oleg A. Igoshin
e-mail: igoshin@rice.edu

Electronic supplementary material is available online at https://doi.org/10.6084/m9.figshare.c.5848997.

THE ROYAL SOCIETY PUBLISHING

The energy cost and optimal design of networks for biological discrimination

Qiwei Yu[1,7], Anatoly B. Kolomeisky[1,2,3,4] and Oleg A. Igoshin[1,2,5,6]

[1]Center for Theoretical Biological Physics, [2]Department of Chemistry, [3]Department of Chemical and Biomolecular Engineering, [4]Department of Physics and Astronomy, [5]Department of Bioengineering, and [6]Department of Biosciences, Rice University, Houston, TX 77005, USA
[7]Lewis-Sigler Institute for Integrative Genomics, Princeton University, Princeton, NJ 08544, USA

QY, 0000-0003-0610-3484; ABK, 0000-0001-5677-6690; OAI, 0000-0002-1449-4772

Many biological processes discriminate between correct and incorrect substrates through the kinetic proofreading mechanism that enables lower error at the cost of higher energy dissipation. Elucidating physico-chemical constraints for global minimization of dissipation and error is important for understanding enzyme evolution. Here, we identify theoretically a fundamental error–cost bound that tightly constrains the performance of proofreading networks under any parameter variations preserving the rate discrimination between substrates. The bound is kinetically controlled, i.e. completely determined by the difference between the transition state energies on the underlying free energy landscape. The importance of the bound is analysed for three biological processes. DNA replication by T7 DNA polymerase is shown to be nearly optimized, i.e. its kinetic parameters place it in the immediate proximity of the error–cost bound. The isoleucyl-tRNA synthetase (IleRS) of *E. coli* also operates close to the bound, but further optimization is prevented by the need for reaction speed. In contrast, *E. coli* ribosome operates in a high-dissipation regime, potentially in order to speed up protein production. Together, these findings establish a fundamental error–dissipation relation in biological proofreading networks and provide a theoretical framework for studying error–dissipation trade-off in other systems with biological discrimination.

1. Introduction

The remarkable fidelity in cellular information processing, including DNA replication [1], transcription [2] and translation [3,4], is realized through a non-equilibrium error-reduction mechanism called kinetic proofreading [5,6]. The proofreading process is dissipative as it introduces an extra energy cost in exchange for improved discrimination against the formation of incorrect products [7]. Besides error and energy dissipation, the reaction speed constitutes another important property of the proofreading system, shown to be optimized in processes such as replication and translation [8–11]. The interplay among speed, accuracy and energy dissipation in systems involving kinetic proofreading (KPR) has been studied in different contexts [8,9,12–26], providing insights to both general KPR networks and specific biological systems achieving discrimination through KPR.

Nonetheless, a fundamental difference distinguishes speed from error and dissipation. In a non-equilibrium steady state, the magnitude of a probability flux is generally affected by the energy levels of both barriers (maxima) and discrete states (minima) of the free energy landscape, but the ratio of fluxes only depends on the barriers (maxima) [23]. In the KPR network, speed is characterized by the magnitude of the product-forming flux, whereas error and dissipation (per product formed) can be expressed as flux ratios. Therefore, speed depends on both minima and maxima, while error and dissipation are determined only by energy maxima. The variation of energy barriers

could create a fundamental constraint (trade-off) between error and dissipation, but speed is decoupled from this trade-off since it can be varied independently by perturbing energy minima. Elucidating this fundamental error–dissipation trade-off is of great importance to the mechanistic understanding of KPR.

Besides the theoretical motivation, the need to quantitatively understand experimentally characterized KPR systems also necessitates the investigation of the error–dissipation bound. Specifically, the trade-offs between speed, error, dissipation and noise in KPR systems have been studied locally, i.e. by examining the change in these characteristic properties due to the variation of a certain rate constant [8,9]. However, different reaction steps may have different priorities in the optimization of characteristic properties. In the KPR network of $tRNA^{Ile}$ aminoacylation, for instance, the amino acid activation step optimizes speed, but the amino acid transfer step optimizes dissipation [22]. A more global approach that examines the effect of simultaneously varying multiple rate constants might be better suited to understand the evolutionary principle and consequence in the placement of the rate constants. This approach reveals a global error–dissipation constraint that illustrates the importance of minimizing the energy cost in $tRNA^{Ile}$ aminoacylation [22] and coronavirus genome replication [27]. The error–dissipation constraint defines a manifold along which the decrease in error will lead to increase in energy cost and *vice versa*. In this sense, it is reminiscent of the concept of the Pareto front in phenotype space due to natural selection [28]. However, much remains unknown about this constraint, including its physical origin and biological importance. Previously, a general matrix method was developed to study the relation between error and energy cost under different constraints [14]. Furthermore, multiple proofreading regimes where accuracy depends on binding energy difference in distinct fashions were discovered [17,18]. More recently, scaling analysis was employed to obtain an asymptotic energy–accuracy–speed relation [19]. The thermodynamic uncertainty relation also imposes a lower bound on the energy dissipation rate [29]. To unify these relations and apply them to understanding biological proofreading systems [4,11,30], it is crucial to develop a general method to obtain the explicit relationship between minimal error and dissipation for biologically relevant models.

In this work, we seek to address these challenges by developing a unified understanding of the fundamental error–dissipation trade-off in general KPR networks. To this end, a theoretical framework is developed with a three-pronged approach unifying the perspectives of chemical kinetics, reaction fluxes and free energy landscape. The KPR process is described by the steady state of a chemical reaction network governed by chemical master equations (CMEs), which can be explicitly transformed into a flux-based formalism enabling the derivation of the exact error–dissipation bound. The bound strictly encapsulates all possible systems, and it can only be approached in the presence of strong non-equilibrium driving in the proofreading cycle and with the fine-tuning of certain flux-splitting ratios. From the free energy landscape perspective, the bound is only determined by the difference of energy barriers between cognate and non-cognate networks, indicating that the trade-off is under kinetic rather than thermodynamic control [24].

The general theoretical framework developed here could be utilized to identify the error–dissipation bound in a large class of KPR networks. We first illustrate its usage in well-recognized models such as Hopfield's scheme and multi-stage proofreading networks with dissociation-based rate discrimination. The methodology's impact, however, is not limited to simplified systems. It is applicable to complex models with arbitrary discrimination factors and multiple intermediates or proofreading pathways. The error–dissipation bound in these systems reveals important physical and biological insights. To demonstrate this, we study three examples whose reaction networks were previously characterized: DNA replication by T7 DNA polymerase, aminoacyl-tRNA selection by *E. coli* ribosome [8], and aminoacylation by *E. coli* isoleucyl-tRNA synthetase (IleRS) [22]. The global parameter sampling confirms that the error–dissipation bound is valid in these systems and that the non-equilibrium driving provided by hydrolyzing energy-rich molecules in the futile cycles is indeed sufficiently large, allowing for the bound to be closely approached. By comparing the native systems with the optimal ones that sit on the error–dissipation bound, we search for general constraints and principles in these biological discrimination systems.

2. Results

2.1. Theoretical formalism

2.1.1. Error and cost in Hopfield's kinetic proofreading scheme

In the classic proofreading scheme proposed by Hopfield [5], the free enzyme E can either bind to the correct substrate (R) forming the cognate complex ER or bind to the incorrect substrate (W) forming EW. The complex then enters an intermediate state ER* or EW*, where it can either generate a product $P_{R/W}$ or undergo proofreading, i.e. resetting without generating any product. Both proofreading and product formation return the enzyme to the unbound state E. This reaction scheme is shown in figure 1*a*. All reactions are pseudo-first-order as fixed concentrations of the substrates and products are maintained. The networks for right and wrong substrates are identical in structure but differ in reaction rates (highlighted in red). In Hopfield's scheme, such difference only exists in dissociation steps, where the rate for the wrong substrate is *f*-fold larger than the rate for the right substrate.

The state of the enzyme at any time t is characterized by a probability distribution vector $\mathbf{P}(t) = [P_{\mathrm{E}}, P_{\mathrm{ER}}, P_{\mathrm{EW}}, P_{\mathrm{ER}^*}, P_{\mathrm{EW}^*}]^T$, where P_{E} denotes the probability of staying in state E., etc. The probabilities are normalized by $\mathbf{1}^T \cdot \mathbf{P} = 1$. The time evolution of the probability distribution is governed by the CME

$$\frac{\mathrm{d}\mathbf{P}}{\mathrm{d}t} = \mathbf{K} \cdot \mathbf{P}, \tag{2.1}$$

where the elements of the transition matrix $\mathbf{K}$ are given by

$$K_{j,i} = \begin{cases} k_{i,j}, & \text{for } j \neq i \\ -\sum_{i \neq m} k_{i,m}, & \text{for } j = i. \end{cases} \tag{2.2}$$

$k_{i,j}$ denotes the rate of transition from state i to state j. Specifically, we study the properties of the system at steady state, which satisfies $\mathbf{K} \cdot \mathbf{P} = \mathbf{0}$ and $\mathbf{1}^T \cdot \mathbf{P} = 1$.

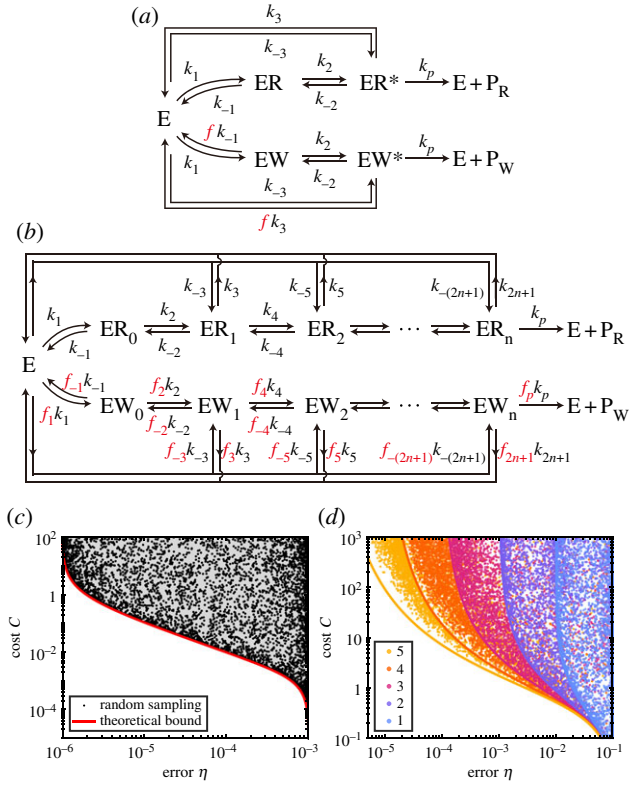

Figure 1. Proofreading schemes and the error–cost trade-off. (*a*) The proofreading scheme proposed by Hopfield [5] with one proofreading pathway and dissociation-based discrimination. (*b*) A generalized proofreading scheme with n proofreading pathways and discrimination factors in all reaction steps. The discrimination factors f and f_i are marked in red, with i labelling the reactions. (*c*) The error–cost relation in the Hopfield scheme (*a*) with $f = 1000$. $N = 2 \times 10^4$ points are shown. Red line: theoretical bound in equation (2.10). (*d*) The error–cost relation in the n-stage dissociation-based-discrimination scheme with $f = 10$ and $n = 1, 2, 3, 4, 5$. Solid lines of the corresponding colour indicate the theoretical bound in equation (2.13). The points are generated with a biased sampling method that prefers points with low error and cost [31]. $N = 3 \times 10^4$ points are shown in total. The thermodynamic constraint is $\ln\gamma = 20$ for (*c*) and $\ln\gamma = 30$ for (*d*).

The steady-state properties of the reaction network can be quantified with two key (dimensionless) properties: error η and proofreading energy cost C. Error is defined as the rate of forming the incorrect product P_W divided by the rate of forming the correct product P_R

$$\eta = \frac{J_W}{J_R}, \tag{2.3}$$

where $J_R = k_p P_{ER^*}$ and $J_W = k_p P_{EW^*}$ are the probability fluxes of forming a correct/incorrect product, respectively. Another important property of such a non-equilibrium reaction system is the free energy dissipation, which could be quantified by the total energy dissipation per correct product formed [9,32,33]:

$$\sigma = \sigma_0 + C(1+\eta)\Delta\mu_{\text{futile}}, \tag{2.4}$$

where $\sigma_0 = \sigma_R + \eta\sigma_W$ is the (fixed) energy cost of making the products and $\Delta\mu_{\text{futile}}$ is the chemical potential difference for the (futile) proofreading cycles, usually corresponding to the hydrolysis of energy-rich molecules such as nucleotide triphosphate (NTP). The cost C is the number of futile hydrolysis reactions per any product formed, calculated by taking the ratio of the total (futile) proofreading flux to the total product formation flux (including both cognate and non-cognate products) [8,13]

$$C = \frac{J_{\text{futile}}}{J_R + J_W}. \tag{2.5}$$

For example, the futile flux in the Hopfield scheme is

$$J_{\text{futile}} = (k_3 P_{ER^*} - k_{-3} P_E) + (k_3 f P_{EW^*} - k_{-3} P_E). \tag{2.6}$$

In this study, we consider σ_0 and $\Delta\mu_{\text{futile}}$ as constants since they are usually fixed by constraints external to the enzyme, such as the chemical potential of substrates, products and other molecules involved in the futile cycle. The chemical potential $\Delta\mu_{\text{futile}}$ is related to the thermodynamic drive of the futile cycle, $\gamma = e^{\Delta\mu_{\text{futile}}} = (k_1 k_2 k_3)/(k_{-1} k_{-2} k_{-3})$ [32,33]. Hence, equation (2.4) indicates that the cost C is a measure of the true (physical) dissipation rate, and the interplay between accuracy and energy dissipation of the proofreading network can be studied by directly investigating the relation between dimensionless numbers C and η. Before analysing their relation, however, we generalize the definitions to other proofreading networks.

2.1.2. Generalizing proofreading schemes

The reaction scheme in figure 1*a* suffers from a few limitations. First, the difference in reaction rates is only present in dissociation steps, while experimental data suggest that disparity in rate constants can exist in any step of the reaction scheme [4,11,30,34–37]. Second, the Hopfield scheme allows for only one proofreading pathway that resets the enzyme, yet many biological systems, such as isoleucyl-tRNA synthetase, involve multiple proofreading pathways [34]. To address these limitations, we study the interplay between error and cost in a generalized scheme that has n proofreading pathways and allows for rate discrimination in all reactions (figure 1*b*). All proofreading pathways reset the enzyme to the initial empty state, thereby resulting in dissipative cycles. The discrimination factors are highlighted in red, with f_i denoting the ratio of rates in step i. Although the network is structurally similar to the McKeithan network [38], the additional proofreading stages here do not involve multiple phosphorylation and therefore dissipate the same amount of free energy. Thus the energy dissipation rate is still given by equation (2.4), with the error η defined as the ratio of the flux forming the incorrect product to that forming the correct product, and the cost C defined as the ratio of the total proofreading flux to the total product formation flux.

In particular, we first illustrate our methodology using direct generalization of the Hopfield scheme in which n proofreading pathways coexist, but the rate discrimination is still limited to dissociation steps with the same factor f. The generalized scheme, which we name the 'n-stage scheme with dissociation-based discrimination' (n-stage DBD), has the same network structure as figure 1*b* with discrimination only in a subset of reactions

$$f_{-1} = f_3 = f_5 = \cdots = f_{2n+1} = f > 1. \tag{2.7}$$

All the other reactions carry no discrimination factor. Rich theoretical insights obtained from studying this scheme would be extended to networks that allow for different discrimination factor in all reactions, especially those describing real biological proofreading processes.

2.1.3. Parameter sampling

The parameter sampling (perturbation) is performed by varying the rate constants $\{k\}$ with fixed discrimination factors $\{f\}$, which is the ratio of a rate constant in the non-cognate network to the rate of the corresponding reaction in the cognate network. For one-stage proofreading systems, the rates $\{k\}$ are sampled from a log-uniform distribution. For multi-stage systems, a sampling method biased towards points with low error and low cost is used [31]. Fixing the discrimination factors is equivalent to maintaining the same energy barrier differences between cognate and non-cognate reactions, thus exerting the same level of kinetic control on substrate discrimination as the original (unperturbed) system. Assuming that the cognate and non-cognate energy barriers correspond to the enzyme in the same conformational state interacting with the respective substrates, perturbation to the enzyme structure would introduce variation to both barriers by the same amount, thus maintaining the same discrimination factor. This is motivated by the commonly used linear free energy relationship that we assume between the cognate and noncognate reactions [39,40].

2.2. Minimal energy cost in Hopfield's proofreading scheme

Figure 1*c* depicts the relation between error and energy cost in the prototypical Hopfield model (figure 1*a*) with rate constants k sampled from a log-uniform distribution over the range $[10^{-5}, 10^{5}]$ and the discrimination factor f kept constant. Each black point represents the error η and cost C of a distinct combination of rate constants $\{k\}$. We find all of the points constrained above a boundary (red line), which effectively defines a Pareto front where no further improvement in error is possible without compromising the cost. Along the boundary, cost decreases monotonically with error, ranging from zero at $\eta_{\mathrm{eq}} = f^{-1}$ to infinity at $\eta_{\mathrm{min}} = f^{-2}$. This is consistent with the previous finding that dissipative proofreading is only necessary if the error needs to be reduced below the equilibrium value f^{-1}, but the error can never be suppressed below f^{-2} [5,6]. We focus on the exact relation between error and cost in the dissipative proofreading regime $\eta \in (\eta_{\mathrm{min}}, \eta_{\mathrm{eq}})$, where the proofreading mechanism becomes necessary.

To aid the mathematical analysis of the error–cost bound, we introduce a flux-based formalism that changes the primary variables of the CME from the probability of each state ($\{P_A\}$, where A labels all possible enzyme states) to the probability fluxes normalized by the correct-product-forming flux. Figure 2*a* illustrates the flux-based formalism of the Hopfield scheme. In the correct half of the network, the normalized fluxes are given by $j_i = J_i/J_{\mathrm{R}}$ $(i = \pm 1, \pm 2)$ and $\beta_{\pm 1} = J_{\pm 3}/J_{\mathrm{R}}$, where J_i is the probability flux of reaction step i and $J_{\mathrm{R}} = k_p P_{\mathrm{R}}$ is the probability flux of forming the right product. To quantify the normalized probability fluxes in the incorrect network, we define an additional error rate η_0 as the ratio of the forward fluxes from EW (ER) to EW* (ER*)

$$\eta_0 = \frac{j'_2}{j_2} = \frac{k_2 P_{\mathrm{EW}}}{k_2 P_{\mathrm{ER}}} = \frac{P_{\mathrm{EW}}}{P_{\mathrm{ER}}}. \tag{2.8}$$

We refer to η_0 as the zeroth-stage error rate as it is the error measured before the first proofreading step. The resulting expressions for the normalized fluxes in the incorrect network are presented in figure 2*a*, with derivation detailed in

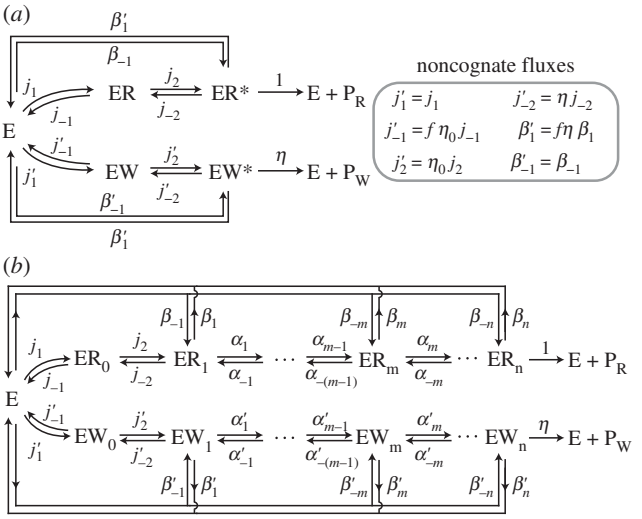

Figure 2. The flux-based formalism for the original Hopfield scheme (*a*) and the *n*-stage proofreading scheme (*b*). The expressions for non-cognate fluxes in (*b*) are given in electronic supplementary material, §II.

electronic supplementary material, §I. In terms of the normalized fluxes, the energy cost is given by

$$C = \frac{(1+\eta f)\beta_1 - 2\beta_{-1}}{1+\eta}. \tag{2.9}$$

The steady-state condition $\mathbf{K}\cdot\mathbf{P} = \mathbf{0}$ in the chemical master equation (CME) translates to a set of stationary conditions in the flux formalism, stipulating that each state must have equal (normalized) fluxes entering and leaving it. The stationary conditions impose four independent constraints on variables $\{j, \beta, \eta\}$, leaving three degrees of freedom. We choose η_0, j_{-2}, and β_{-1} as free variables with respect to which the cost is minimized. Moreover, η_0 is bounded by the equilibrium error rate, namely $\eta_0 > \eta_{\mathrm{eq}} = f^{-1}$, where the minimum is only achieved in the limit of fast binding and unbinding between the free enzyme and the substrate. We discover that the minimum cost is achieved when $\eta_0 \to f^{-1}$ and j_{-2}, $\beta_{-1} \to 0$ (see electronic supplementary material, §I for detailed derivation)

$$C_{\mathrm{min}}(\eta, f) = \frac{1-\eta^2 f^2}{(1+\eta)(\eta f^2 - 1)}, \tag{2.10}$$

which exactly bounds all data points found in numeric sampling (figure 1*c*, red line). Notably, as η decreases within the range $\eta \in (f^{-2}, f^{-1})$, the cost C_{min} increases monotonically and exhibits a divergence at the minimum error. This can be compared with the error–cost bound in multi-stage proofreading schemes, where the cost diverges much faster toward a smaller error minimum.

The conditions for minimizing the cost reveal how the probability fluxes should be arranged for the scheme to be energetically optimal without impairing the accuracy. The first condition, $\eta_0 = f^{-1}$, indicates that the reactions between E, ER and EW are in fast equilibrium. Hence, the ratio of probabilities P_{EW} and P_{ER} is determined by the ratio of their respective association constants with the enzyme, which is f^{-1}. In many biochemical systems, the first step corresponds to the binding between enzyme and substrates, which is indeed in fast equilibrium compared to the

subsequent catalytic reactions. The second condition, $j_{-2} \to 0$, indicates that this reverse flux only increases the energy dissipation. To better understand it, let us imagine a perturbation redirecting j_{-2} to forming the correct product and j'_{-2} to forming the incorrect product. This perturbation will not change the error rate since $j'_{-2}/j_{-2} = \eta$. The stationary conditions also remain unaffected since the product-forming fluxes return to the free enzyme state, which is in fast equilibrium with states ER and EW. In this way, however, we have generated more products without increasing the futile fluxes and thereby reduced the cost. Therefore, vanishing fluxes j_{-2} and j_{-2}' are always energetically favourable. The third condition, $\beta_{-1} \to 0$ deals with the reverse proofreading fluxes. Although these fluxes seem to reduce the dissipation, they also significantly increase the error: going directly from E to ER*/EW* introduces error $\beta_{-1}'/\beta_{-1} = 1$, which is always higher than the error $j_2'/j_2 = \eta_0$ from going through intermediate states ER/EW. The condition of vanishing β_{-1} indicates that the reduction in dissipation due to reverse proofreading is outweighed by the increase in forward proofreading fluxes needed to mitigate the increase in error.

To summarize, the optimal proofreading system consists of three independent steps: first, the error is reduced to $\eta_0 = (P_{\mathrm{EW}}/P_{\mathrm{ER}}) \to f^{-1}$ through the fast equilibrium in the binding and unbinding between the enzyme E and the substrate R/W; second, the complex undergoes an activation step (from ER/EW to ER*/EW*), which is almost irreversible; third, the error is reduced from η_0 to η with a proofreading mechanism that is also almost irreversible. Note that the activation and proofreading steps cannot be strictly irreversible due to the thermodynamic constraint $\gamma = (k_1k_2k_3)/(k_{-1}k_{-2}k_{-3})$. However, this constraint only increases the minimum cost by a small correction term of the order $\gamma^{-1/2}$ (see electronic supplementary material, §I), which is usually negligible in real networks since $\gamma \gg 1$ (for instance, $\gamma = \mathrm{e}^{20}$ in the DNA replication network).

The key factor that characterizes the intensity of proofreading is the partition ratio of proofreading over product formation

$$\beta_1 = \frac{J_3}{J_R} = \frac{1 - \eta f}{\eta f^2 - 1}. \tag{2.11}$$

Under the optimal setting, the ratio decreases monotonically with η, indicating one-to-one monotonic correspondence between the optimal proofreading intensity and the desired accuracy. Networks that are non-optimal always have a larger partition ratio compared to the optimal network with the same error rate. The significance of this ratio will be further illustrated in networks with multiple proofreading pathways.

2.3. Minimum energy cost in multi-stage schemes with dissociation-based discrimination

The natural generalization of the Hopfield scheme is to have multiple proofreading pathways while still localizing the discrimination to dissociation steps. Hence, we study the so-called n-stage dissociation-based-discrimination (DBD) scheme, with network structure shown in figure 1*b* and discrimination factors given by equation (2.7). By preferentially sampling systems with low error and proofreading cost [31], we identify error–cost boundaries for systems with different numbers of proofreading pathways n (figure 1*d*). For each system, the minimum dissipation starts from zero at $\eta_{\mathrm{eq}} = f^{-1}$ and increases as the error decreases before diverging to infinity at $\eta_{\min} = f^{-n-1}$. The same minimum error has also been obtained with a graph theoretic approach [41].

Next, we analyse the error–cost bound in the n-stage DBD scheme with the flux-based formalism (figure 2*b*). For each stage m ($m = 1, 2, \ldots, n$), we define $\alpha_{\pm m}$ as the normalized forward/backward fluxes and $\beta_{\pm m}$ as the normalized proofreading/reverse proofreading fluxes. The m-stage error η_m is defined as the ratio of the forward fluxes going from $\mathrm{EW_m}$ ($\mathrm{ER_m}$) to $\mathrm{EW_{m+1}}$ ($\mathrm{ER_{m+1}}$). The final error is $\eta = \eta_n$. These η characterize how the error is sequentially reduced from $\eta_0 = \eta_{\mathrm{eq}}$ to $\eta_n = \eta$ through n proofreading steps. Similar to the case of the original Hopfield scheme, the normalized fluxes in the noncognate network can be expressed in terms of α, β, η, and f (see electronic supplementary material, §II). Through mathematical induction, we found that the proofreading cost in a n-stage DBD scheme C_n is bounded by

$$C_n \geq \frac{(1 + f^{-1})(f - 1)^n}{1 + \eta} \prod_{m=1}^{n} \frac{\eta_m}{\eta_m f - \eta_{m-1}} - 1, \tag{2.12}$$

whose equality condition is $\alpha_{-i}, \beta_{-i} \to 0$ for $i = 1, 2, \ldots, n$, $j_{-2} \to 0$, and $\eta_0 = f^{-1}$. Effectively, the system is optimal when the binding step is in fast equilibrium and the chemical reactions towards product formation or proofreading are nearly irreversible. Complete irreversibility is precluded by the thermodynamic constraint, which increases the minimum cost by a correction term of the order $\gamma^{-1/(n+1)}$ (see electronic supplementary material, §II). The intermediate error rates $\{\eta_m\}$ characterize the distribution of proofreading burden between different reaction stages, which can be further optimized. We introduce $\lambda_m = \eta_{m-1}/\eta_m > 1$ to quantify the increase in accuracy at stage m. These ratios are constrained by $\prod_{m=1}^{n} \lambda_m = \eta_0/\eta = (f\eta)^{-1}$. The product under the Π notation in equation (2.12) is thus given by $\prod_{m=1}^{n} (f - \lambda_m)^{-1}$. Due to symmetry, the optimal system has equal λ at all stages, i.e. $\lambda_m = (\eta_0/\eta_n)^{1/n} = (f\eta)^{-1/n}$, which leads to the expression for minimum energy cost (also see electronic supplementary material, §II):

$$C_{n,\min}(\eta, f) = \frac{(f - 1)^n (f + 1)}{((\eta f)^{1/n} f - 1)^n} \frac{\eta}{1 + \eta} - 1. \tag{2.13}$$

Indeed, this boundary constraints all points on the error–cost plane for each n (solid lines, figure 1*d*). In the optimal scheme, the reduction of error is carried out sequentially, with each proofreading step reducing the error by a factor of $\eta_m/\eta_{m-1} = (f\eta)^{1/n}$. This implies that the burden of correcting errors is evenly distributed across n proofreading pathways without any preference to early or late pathways. Notably, the minimum cost exhibits nth-order divergence in the limit of minimum error (i.e. $C_{\min} \propto (\eta - \eta_{\min})^{-n}$), which is much stronger than the first-order divergence in the original Hopfield scheme.

The error–cost trade-off in the n-stage DBD scheme is controlled by two parameters: the discrimination factor f and the number of proofreading pathways n. Increasing either f or n reduces the overall minimum error $\eta_{\min} = f^{-n-1}$ as well as the minimum energy cost at any given error rate (equation 2.13). They correspond to two error-correcting strategies: enhancing the discriminating capability of each individual proofreading pathways or redistributing the burden of error

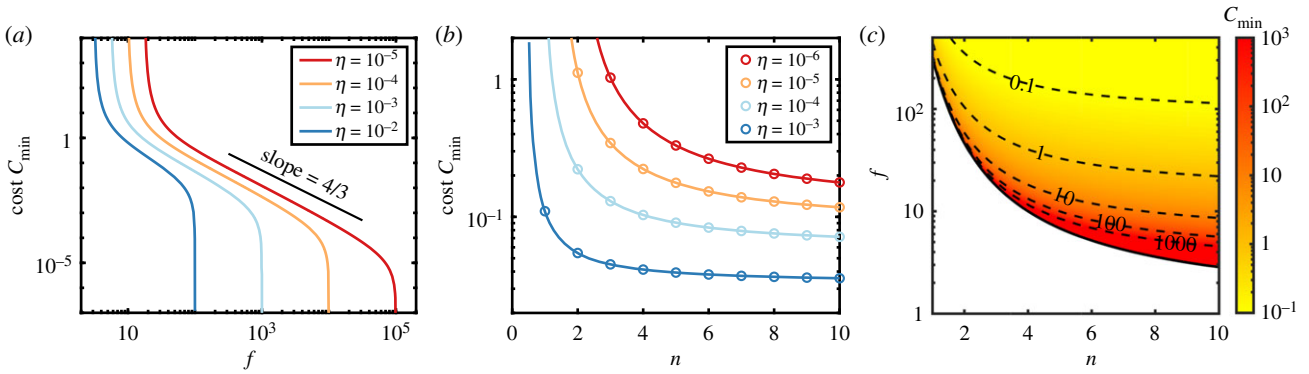

Figure 3. Energy cost in the n-stage dissociation-based-discrimination scheme can be reduced by increasing n or f. (*a*) For a given error rate, the minimum cost decreases with the discrimination factor f. $n = 3$. η is specified in the legend. (*b*) For a given error rate, the minimum cost decreases with the number of proofreading pathways n. Here, $f = 100$ and η is specified in the legend. (*c*) Heatmap of C_{min} as a function of f and n at a fixed error $\eta = 10^{-5}$. The area below the black line $\eta = f^{-(n+1)}$ is strictly inaccessible.

correction to additional pathways. In real biochemical systems, increasing n often requires the enzyme to have multiple reaction/proofreading domains, and the discrimination factor f is determined by the free energy landscape of the underlying biochemical reactions. Here, we analyse the kinetic effects and defer the implication in specific biochemical contexts to §3. Figure 3*a* studies the relation between the minimum cost and the discrimination factor f. For any fixed n and η, the minimum cost diverges to infinity when f is so small that the system operates near the minimum error and approaches zero when f tends to η^{-1}, allowing the system to operate in the equilibrium discrimination regime. In the intermediate error range, however, we find the minimum cost decreasing, with f following a power law with exponent $(1 + n^{-1})$ (see electronic supplementary material, §II for derivation). Increasing f in this range results in a non-diminishing return in the decrease of cost. By contrast, although increasing n also reduces the minimum cost, the benefit becomes marginal when n is large, and the minimum cost never decreases to zero even when n tends to infinity (figure 3*b*). These two effects can be summarized in figure 3*c*, which depicts how the minimum cost depends on n and f for a given error rate. The orientation of the (dashed) cost contours demonstrates that the cost decreases with both n and f but varies more rapidly along the f direction. The solid black line shows the error minimum, where the cost diverges.

2.4. The optimal scheme is kinetically controlled

The intermediate error rates η_m in the optimal n-stage DBD system form a geometric series, where each proofreading stage reduces the error by the same factor. This is achieved by a specific combination of rate constants. In particular, each intermediate state in the optimal scheme has the equal ratio of partition between proofreading (resetting to E) and moving forward to the next intermediate state along the product formation pathway:

$$a_m = \frac{\beta_m}{\alpha_m} = \frac{1 - (\eta f)^{1/n}}{f(\eta f)^{1/n} - 1} = \frac{k_{2m+1}}{k_{2m+2}}. \tag{2.14}$$

In fact, this partition ratio reveals how features of the free energy landscape shape the fundamental trade-off between accuracy and energy dissipation. To illustrate this, we construct a simple kinetic model (figure 4*a*) that elucidates the flux dynamics in optimal multi-stage proofreading networks. The f-fold discrimination due to the fast equilibrium in the binding steps is captured by the two reactions in the blue dashed box, which create an f^{-1}-fold difference in the production of EW_1 compared to ER_1. All the subsequent intermediate states are assigned with a reaction rate κ_i (or equivalently a time scale $\tau_i = \kappa_i^{-1}$) and a partition ratio a that is identical for all proofreading pathways. We also assign κ_0 to the initial steps. By allowing for completely irreversible reactions, this model only calculates the leading order term of cost in the large γ limit. The steady-state probability distribution of this model is obtained by directly solving the CME (see electronic supplementary material, §III), which reveals that both error η and cost C are completely determined by only f and a. They are independent of all the κ_i ($i = 0, 1, \ldots, n$). As illustrated in figure 4*b*, increasing a continuously from zero to infinity drives the system from the equilibrium discrimination regime with no proofreading cost ($\eta_{eq} = f^{-1}$ and $C = 0$) towards the non-equilibrium limit with highest accuracy and diverging cost ($\eta \to \eta_{min} = f^{-n-1}$ and $C \to +\infty$). Varying κ has no effect on either error or cost. We also find that the intermediate error rate η_m forms a geometric series in the same way as seen in the n-stage DBD scheme, and eliminating a from the expression of η and C recovers the error–cost bound in equation (2.13). Therefore, the system sits on the optimal error–cost boundary as long as all proofreading stages share the same partition ratio a. Moreover, the ratio a functions as a tuning parameter that only moves the system along the Pareto front of the error–cost trade-off (i.e. theoretical bounds in figure 1*c*,*d*). This relation is depicted in figure 4*c*, where each value of a corresponds to the optimal scheme for a different error rate and all the systems obtained in the previous parameter sampling fall within the grey accessible region above the optimal bound.

It is not a coincidence that both error and cost are determined by the partition ratio a but not rates κ_i. In fact, the deeper explanation lies in the different features of the underlying free energy landscape captured by these rates. Previous work has shown that any quantities that can be expressed as ratios of stationary fluxes, including both η and C, are invariant against perturbation of the energy level of discrete states (minima on the free energy landscape) and only affected by perturbation of the energy barriers (maxima) [23]. Expressing

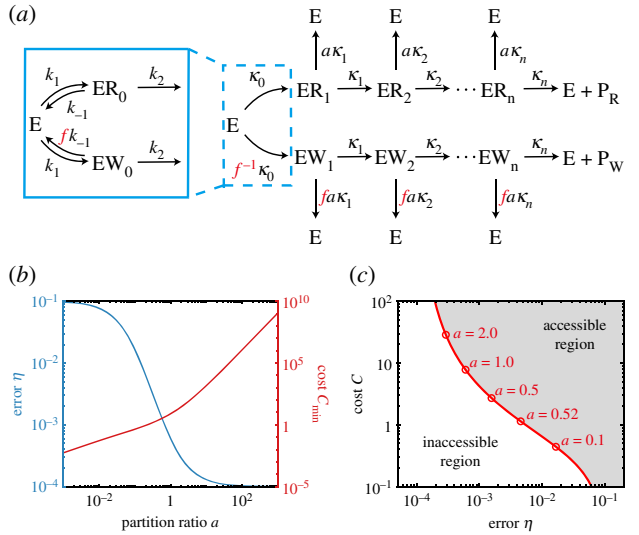

Figure 4. The kinetics of an optimal proofreading network with only dissociation-based discrimination is captured by a simple kinetic model. (*a*) Minimal kinetic model for the *n*-stage proofreading scheme. (*b*) The partition ratio a serves as a controlling parameter simultaneously tuning error η and cost C. Parameters are $n = 3$ and $f = 10$. (*c*) Varying a in the minimal model corresponds to moving the system along the optimal front in the error–cost trade-off, which separates the accessible and inaccessible regions.

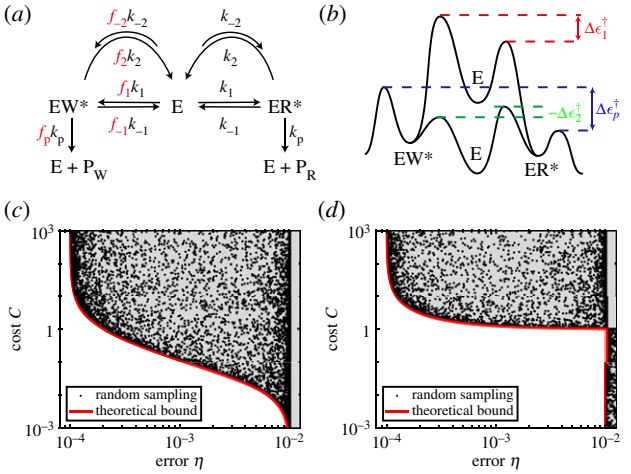

Figure 5. Michaelis–Menten reaction scheme with dissipative resetting. (*a*) The kinetic scheme. The discrimination factors f are highlighted in red. (*b*) The free energy landscape of the kinetic scheme. (*c*,*d*) Error and energy cost of sampled networks (black dots) with two different set of discrimination factors. Red lines: theoretical boundary given by equation (2.16). (*c*) $f_1 = 10^{-2}$, $f_{-1} = 1$, $f_2 = 10^2$, $f_p = 1$, $f_{-2} = 1$; (*d*) $f_1 = f_p = 1$, $f_{-1} = 10^2$, $f_2 = 10^4$, $f_{-2} = 10^2$. The chemical potential for the futile cycle is set to $\Delta\mu = 20\ k_BT$ ($\ln\gamma = 20$). $N = 2 \times 10^4$ points are shown in (*c*,*d*).

κ_m and a in terms of the energy levels [42], we find

$$\kappa_m \propto e^{\epsilon_m - \epsilon^\dagger_{m,m+1}} \quad \text{and} \quad a\kappa_m \propto e^{\epsilon_m - \epsilon^\dagger_{m,p}}, \tag{2.15}$$

where ϵ_m is the energy of state ER_m, $\epsilon^\dagger_{m,m+1}$ is the free energy barrier between ER_m and ER_{m+1}, and $\epsilon^\dagger_{m,p}$ is the free energy barrier in the proofreading step (from ER_m to E). Hence, a is associated with the difference in energy barriers $(\epsilon^\dagger_{m,m+1} - \epsilon^\dagger_{m,p})$, which is key to the kinetic control of stationary flux ratios [23]. In contrast, perturbing κ_m is equivalent to varying the energy level of ER_m, which is irrelevant to any ratio of stationary fluxes, such as η and C. These results reinforce the argument that KPR is kinetically controlled [24] and highlights the importance of the partition ratio in both investigating natural biological proofreading systems and engineering synthetic biological systems with high selectivity.

2.5. Networks with arbitrary discrimination factors

To elucidate the biological implications of the error–dissipation trade-off studied so far, we need to generalize it to networks that allow for disparity in the rate constants in all reaction steps (figure 1*b*). To illustrate the idea for generalization, we first study the classic Michaelis–Menten scheme with the addition of a resetting reaction (figure 5*a*, henceforth named MM-with-proofreading), which could be regarded as a basic building block that makes up more complex proofreading networks (e.g. with multiple proofreading pathways). The resetting cycle is driven by the cycle chemical potential difference $\Delta\mu = k_BT\ln[k_1k_2/(k_{-1}k_{-2})]$, which allows for increasing accuracy at the cost of energy dissipation. The disparity in reaction rates is quantified by the discrimination factors f_i (highlighted in red; i labels the reaction steps), which obey the thermodynamic constraint $f_1f_2 = f_{-1}f_{-2}$. Following the previous methodology, we define error η as the ratio of the product formation fluxes and cost C as the sum of the futile fluxes normalized by the total product formation flux.

Before studying the accuracy–energy trade-off, we first identify the parameter regime where dissipative proofreading becomes relevant. The resetting only improves the accuracy when it dissociates EW* more readily than ER*. Hence, f_2 should be sufficiently large for proofreading to be effective. In fact, we find proofreading meaningful only when f_2 is greater than both f_{-1} and f_p, which is explained as following. First, the dissipative resetting is only useful when it creates more bias than the non-dissipative dissociation step k_{-1}, which requires $f_2 > f_{-1}$; otherwise using only the equilibrium discrimination would be more accurate and less dissipative. Second, the proofreading mechanism should proportionally dissociate more wrong complexes compared to the right ones, which requires the non-cognate network to have a larger proofreading-to-product-formation partition ratio, namely $k_{2,W}/k_{p,W} > k_{2,R}/k_{p,R}$. This is equivalent to stipulating $f_2 > f_p$. With these two conditions, we find the system capable of achieving the minimum error $\eta_{\min} = f_1f_p/f_2$, which is lower than the minimum error of equilibrium discrimination $\eta_{eq} = \min(f_1, f_1f_p/f_{-1})$, calculated in the absence of proofreading ($k_{\pm 2} = 0$). Therefore, the trade-off between accuracy and energy dissipation is analysed in the error range $\eta \in (\eta_{\min}, \eta_{eq})$, which can only be realized with proofreading. With the flux-based method, it can be shown that for a given error rate, the energy cost C is minimized when the reverse reaction rates $k_{-1,-2}$ become vanishing (see electronic supplementary material, §IV). The minimum cost reads

$$C_{\min} = \frac{(f_1 - \eta)(1 + \eta(f_2/f_p))}{(1 + \eta)(\eta(f_2/f_p) - f_1)}. \tag{2.16}$$

To examine this bound numerically, we sample all reaction rates in the MM-with-proofreading scheme with fixed discrimination factors and chemical potential. Figure 5*c*,*d* present the sampling results for two different sets of

discrimination factors. Consistent with theory, all sampled systems reside above the boundary given by equation (2.16) (red lines). The cost diverges to infinity as the error approaches minimum. Towards the $\eta \to \eta_{\rm eq}^-$ limit, however, the minimum cost approaches zero in the case of figure 5*c* but converges to a positive value in figure 5*d*. As zero proofreading cost is expected in the equilibrium regime ($\eta > \eta_{\rm eq}$), the discontinuity in figure 5*d* indicates a sudden change of the optimal rate configuration during the transition from the non-equilibrium regime to the equilibrium regime. In the absence of proofreading, the minimum error is achieved by making either k_1 or k_p rate-limiting, which leads to error rates of $\eta = f_1$ or $\eta = f_1 f_p / f_{-1}$, respectively. $\eta_{\rm eq}$ corresponds to the more accurate one of these two configurations. In the optimal scheme in the non-equilibrium regime, nonetheless, the rate k_{-1} is always vanishing as seen in the cost minimization condition derived above. Hence, there is a discontinuous regime change if $f_p < f_{-1}$, where the $k_{\pm 1}$ step is in fast equilibrium on the equilibrium side and almost irreversibly driven forward on the non-equilibrium side, resulting in the discontinuous error–cost relation as seen in figure 5*d*. If $f_p \geq f_{-1}$, however, k_{-1} is vanishing on both sides of $\eta_{\rm eq}$, and the error–cost bound is continuous at $\eta_{\rm eq}$, which is the case in figure 5*c*. This regime change is a feature present only in networks whose rate discrimination is not limited to dissociation steps. Other than the discontinuity at $\eta_{\rm eq}$, the error–cost bound has the same quantitative profile as the original Hopfield scheme.

It is remarkable that out of all the discrimination factors, the error–cost relation (equation 2.16) is only controlled by f_1 and the ratio f_2/f_p. This can be understood from the perspective of free energy landscape (figure 5*b*), where previous analysis has shown that both error and cost are determined solely by the energy barriers. We denote the energy barriers by $\epsilon^\dagger_{\lambda,{\rm R/W}}$, where $\lambda \in \{1, 2, p\}$ labels the reaction and R/W distinguish the right/wrong half of the network. The discrimination factors are associated with the difference of energy barriers for cognate and non-cognate substrates

$$f_1 \propto {\rm e}^{-\Delta\epsilon_1^\dagger}, \quad \frac{f_1 f_2}{f_{-1}} \propto {\rm e}^{-\Delta\epsilon_2^\dagger} \quad \text{and} \quad \frac{f_1 f_p}{f_{-1}} \propto {\rm e}^{-\Delta\epsilon_p^\dagger}, \tag{2.17}$$

where $\Delta\epsilon^\dagger_\lambda = \epsilon^\dagger_{\lambda,{\rm W}} - \epsilon^\dagger_{\lambda,{\rm R}}$ denotes the difference between energy barriers (figure 5*b*). Hence, the ratio f_2/f_p, which equals to the partition ratio in the non-cognate network divided by the partition ratio in cognate network, is proportional to ${\rm e}^{\Delta\epsilon_p^\dagger - \Delta\epsilon_2^\dagger}$. In other words, the fundamental error–dissipation trade-off is governed only by the energy barrier differences $\Delta\epsilon_1^\dagger$ and $(\Delta\epsilon_p^\dagger - \Delta\epsilon_2^\dagger)$. Moreover, the error–cost bound in more complex biological proofreading networks can be readily derived by identifying the equivalents of f_1 and f_2/f_p since they already capture all the relevant features of the energy landscape. Next, we apply this technique to three real proofreading systems with parameters provided in previous studies [8,9,22] and discuss biological implications.

2.6. Error–cost trade-off in real biological networks

To illustrate the robustness of the bound, we apply our theoretical framework to three real biological proofreading networks, where numerical sampling confirms that the bound formulated with our theory tightly constrains the error and cost of all systems sampled. The position of the native systems compared to the bound reveals the relative importance in the evolutionary optimization of functionalities including speed, accuracy and dissipation in KPR systems.

We start with DNA replication by T7 DNA polymerase (DNAP), which employs a one-cycle proofreading mechanism [8,10]. Its reaction network is similar to the MM-with-proofreading scheme with an additional intermediate state in the proofreading step. Since the proofreading step is irreversible at the bound, the presence of this intermediate state does not affect the validity of the error–cost bound given in equation (2.16) (see electronic supplementary material, §V for details). Figure 6*a* presents the result of sampling all rate constants while fixing the discrimination factors. Indeed, all the sampled systems fall exactly above the theoretical bound outlined by the red line. Notably, the native system (green diamond) resides close to the boundary. The energy cost C for the native system is only 4.3% larger than the minimum possible cost at the native error rate, which means that only a small portion of futile hydrolysis is excessive. The energy efficiency of the DNA polymerase could also be assessed by the proofreading-to-product-formation partition ratio $a = k_2/k_p = 8 \times 10^{-4}$, which is close to its minimum possible value $a_{\rm min} = 4.5 \times 10^{-4}$ for the optimal system at the native error rate. In analogy to the original Hopfield scheme, the DNAP network approaches the error–cost bound by driving both polymerization and proofreading irreversibly forward. Indeed, we find the forward/backward polymerization rate ratio to be $k_1/k_{-1} = 250 \gg 1$, and the rate ratio in proofreading to be $(k_2 k_3)/(k_{-2} k_{-3}) = 2 \times 10^6 \gg 1$. These reactions are driven forward by the non-equilibrium driving $\Delta\mu = 20 k_B T$ in the futile cycle, which comes from hydrolyzing one dNTP (deoxynucleoside triphosphate) molecule. Going below the native error rate, the system has the potential of reducing the error by more than two orders of magnitude (from 10^{-8} to 10^{-10}). However, this will lead to about one futile hydrolysis per product formed ($C \approx 1$), effectively doubling the total energy dissipation of DNA replication. Hence, it is possible that further increase in replication accuracy is prevented in order to avoid potentially disadvantageous excessive energy dissipation.

Next, we consider the aminiacyl-tRNA (aa-tRNA) selection process by ribosome during translation [8,43]. This network also has only one proofreading pathway, and the error–cost bound is fully captured by equation (2.16) with f_1 replaced by the minimum error achievable in steps prior to proofreading and f_2 replaced by the discrimination in the proofreading step in this network (see electronic supplementary material, §V for details). The error–cost bound is also obtained for a more detailed ribosome model [44], which demonstrates that taking additional intermediate states into account does not change the form of the bound (see electronic supplementary material, §V for details). As shown in figure 6*b*, the bound (red line) exactly encapsulates all sampled systems on the error–cost plane. The vertical part of the bound indicates the minimum error for equilibrium discrimination $\eta_{\rm eq}$, above which proofreading becomes unnecessary and the minimum cost is zero. Unexpectedly, the native system resides within this equilibrium regime, seemingly suggesting that the proofreading mechanism is redundant. The error–cost trade-off has also been analysed for the error-prone and hyperaccurate mutants of the ribosome [43], whose native error rates are also larger than $\eta_{\rm eq}$ (see electronic supplementary material, §V).

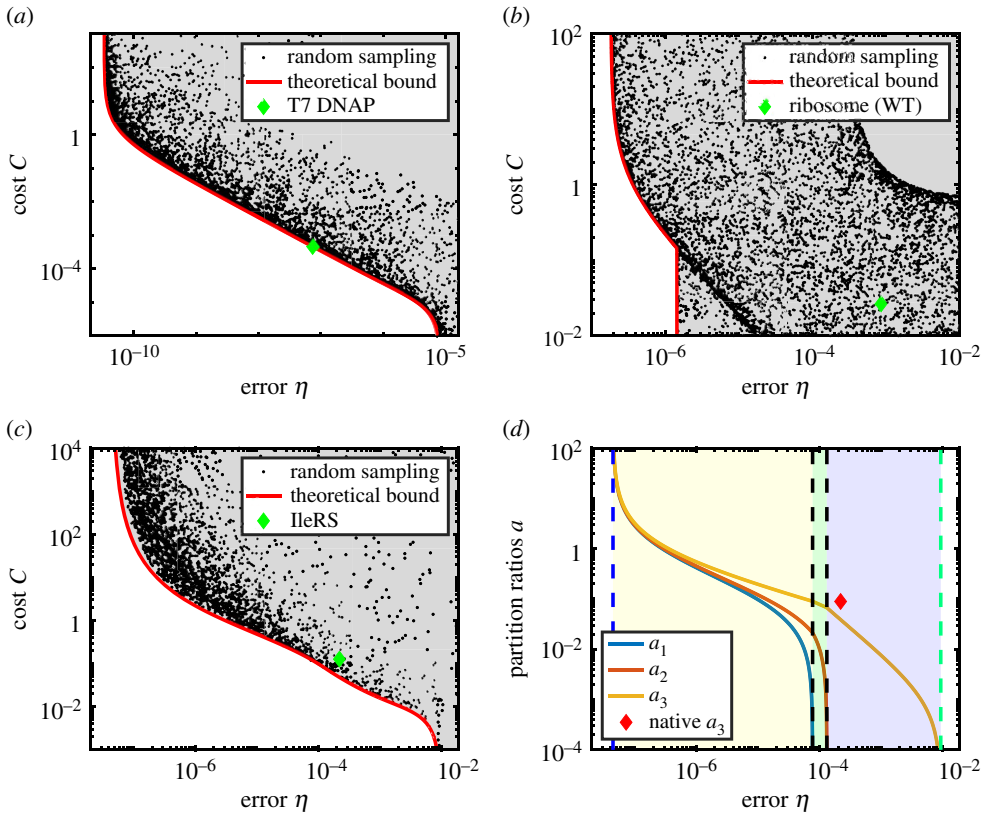

Figure 6. Results in biological networks involving proofreading (see electronic supplementary material, §V for details of the reaction schemes). (*a*) The error–cost relation in the T7 DNA polymerase network due to sampling all parameters. (*b*) The error–cost relation in the protein synthesis network. (*c*) The error–cost relation in the isoleucyl-tRNA synthetase (IleRS) network. All rate constants sampled obey their original thermodynamic constraints. (*d*) The optimal (solid lines) and native (red diamond) partition ratios in the IleRS network. The blue dashed line indicates the minimum error and the green dashed line indicates minimum error for discrimination without dissipation. The black dashed lines show thresholds where a_1 and a_2 vanish. The yellow, green and blue shades indicate phases of $n = 3, 2, 1$.

To understand what prevents the ribosome from realizing the theoretical possibility of maintaining the native error rate without proofreading, we remove both forward and backward proofreading reactions ($k_{\pm 2} = 0$) and examine adjustments in the other rate constants required to achieve the native error rate. Theoretically, the error is minimized when the product formation step is rate-limiting. It requires a time-scale separation where k_p, which corresponds to the accommodation of the aa-tRNA into the A site of the large subunit and the subsequent peptidyl-transfer, is much smaller than the rate constants of all the preceding reactions. Experimental measurements, however, found k_p comparable to the rates of preceding reactions [43]. It is threefold smaller than the GTP hydrolysis rate and fivefold smaller than the binding rate of the ternary complex containing tRNA, EF-Tu (elongation factor Tu) and GTP. Restoration of the native error rate would require reducing k_p and/or increasing other rate constants. On the one hand, reducing k_p directly slows down the speed of protein synthesis and eventually the speed of cell growth, especially since translation is suggested as a rate-governing process in bacterial growth [45]. If all the other rate constants remain invariant, k_p needs to be decreased 700-fold to recover the native error rate. This leads to significant decrease in the growth rate, which would seem evolutionarily detrimental. On the other hand, amplification of the rates of the preceding reactions faces physical limitations. For example, the rate of ternary complex binding is already close to its upper limit, which corresponds to diffusion-limited reaction [46], rendering further rate increase impossible. Therefore, it would seem that the condition to maintain the native error rate without proofreading could not be fulfilled without sacrificing the overall rate of protein synthesis and bacterial growth. The analysis above indicates that reaction speed becomes an important factor when considering real proofreading networks, where the low-cost equilibrium discrimination regime permissible in the theory could be kinetically prohibited. Therefore, the proofreading mechanism is still necessary in the native system, contributing to a 20-fold increase in the translation fidelity [43]. The above analysis indicates that the minimum dissipation for protein translation is limited by the speed constraints rather than the error–cost trade-off.

To extend our analysis to multi-stage proofreading networks, we study the reaction network for IleRS in *E. coli* [22]. The enzyme pairs $\mathrm{tRNA}^{\mathrm{Ile}}$ with the cognate amino acid isoleucine (Ile) by discriminating it against a chemically similar amino acid, valine (Val) [34]. The network has the structure of figure 1*b* with $n = 3$ proofreading stages. The error–cost bound could be derived by generalizing the bound in the MM-with-proofreading scheme with the mathematical induction method used in the n-stage DBD scheme (see electronic supplementary material, section V). Figure 6*c* presents the error–cost relation due to the rates sampling, demonstrating that all systems sampled fall above the theoretical error–cost bound. The native system falls within the non-equilibrium discrimination regime (i.e. $\eta < \eta_{\mathrm{eq}}$). Similar to T7 DNA polymerase, the enzyme resides close to the boundary, whose cost is 2.6-fold of the minimum cost required to

maintain the same error rate. In terms of the energy dissipated per Ile-tRNA^{Ile} formed (σ), the dissipation of the native system is only slightly (less than 20%) larger than the optimal system. This finding reaffirms that IleRS is energetically efficient [22].

The reason why the dissipation could not be further reduced could be explained by analysing the optimal schemes corresponding to the bound. In contrast to the n-stage DBD scheme where all proofreading pathways are equally leveraged, the IleRS network has three different proofreading regimes characterized by different number of 'effective' proofreading pathways with nonzero proofreading fluxes. To understand this, we calculate the optimal partition ratios $a_{1,2,3}$ as a function of error η (figure 6*d*). The full error range $\eta \in (\eta_{\min}, \eta_{eq})$ can be categorized into three phases (represented by different shades in figure 6*d*) by the number of nonzero partition ratios. When the error is sufficiently small, all three stages need to be functional (yellow phase, $n = 3$). Due to the different discrimination factor, however, the partition ratios are different among the three stages. The post-transfer proofreading pathway, which has the most discrimination, has the largest partition ratio a_3. Conversely, the first pre-transfer proofreading pathway has the smallest partition ratio a_1. These partition ratios decrease as the error is increased until a threshold (left black dashed line) is reached where $a_1 \to 0$. Further increase in error leads to a negative a_1, which is prohibited since the rate constants are always positive. Negative a_1 is also thermodynamically impossible since all proofreading pathways have the same non-equilibrium driving γ, which precludes coexistence of proofreading and anti-proofreading in different pathways (otherwise there will be cyclic flux on a reaction loop with no driving, such as the loop ER_1–E–ER_2 in figure 1*b*). Therefore, the first pre-transfer proofreading pathway is turned off (namely $a_1 = 0$) for error larger than this threshold. Similarly, there is a second threshold (right black dashed line) where $a_2 \to 0$, turning off the second pre-transfer proofreading pathway. The optimal system effectively operates in a two-stage proofreading regime for error rates between the two thresholds (green phase, $n = 2$) and in a one-stage regime for error larger than the second threshold (blue phase, $n = 1$). The native system (red diamond) resides in the one-stage regime where the optimal scheme utilizes only the post-transfer proofreading mechanism. The native partition ratios a_1 and a_2 are indeed negligibly small, while the native a_3 is about two-fold of its optimal value, accounting for the increased cost. The increased a_3 can in fact be attributed to steps before proofreading, where the actual error rate is about twice of the minimum error η_{eq}. Reducing this error rate requires decreasing the rate of amino acid activation, which will decrease the speed of product formation. This is consistent with the previous trade-off analysis on the activation rate, which indicated that the reaction optimizes speed over energy dissipation [22]. Therefore, similar to the case of translation, the native IleRS system's deviation from the optimal bound could be explained by the speed requirement. Moreover, the small partition ratios in pre-transfer editing ($a_{1,2}$) could be a result of selective pressure to reduce the energy dissipation in aminoacylation. It is possible that after the early emergence of the CP1 editing domain, which is responsible for post-transfer editing [47], the pre-transfer editing activity ($a_{1,2}$) evolved to decrease, allowing errors to be corrected more efficiently in post-transfer editing (a_3). Taken together, the analyses of translation and aminoacylation seem to suggest that *E. coli* places high priority on optimizing the rate of protein synthesis and therefore growth rate, even at the expense of higher proofreading cost.

3. Discussion

3.1. The error–dissipation trade-off is kinetically controlled

We have analysed the error and energy cost of kinetic proofreading in a large class of reaction networks whose dynamics are governed by the CME. In terms of methodology, we propose a formalism whereby the probability fluxes serve as the primary variables of interest. The flux-based formalism complements the CME formalism and provides a useful mathematical device for understanding the flux kinetics in reaction networks, especially those with symmetric and branching structures. Applying the flux-based formalism to models of biological proofreading could reveal important biological insights. In terms of physical interpretation in the context of the free energy landscape, we demonstrate that both error η and cost C depend only on the energy barriers rather than the energy levels of discrete states (kinetic control). More precisely, the energy barriers determine error and cost through the partition ratio a. Having uniform partition ratios in different proofreading stages is necessary for optimizing the error–cost relation in the n-stage DBD scheme, and the magnitude of the partition ratio determines the extent to which error or dissipation is prioritized in their trade-off. In the minimal multi-stage proofreading scheme (figure 4*a*), it is further demonstrated that the energy level of discrete states is irrelevant to both error and cost, and that the uniform partition ratio parameterizes the system's position along the error–cost bound (figure 4*c*).

These theoretical analyses suggest experimental characterization of reaction fluxes rather than the rate constants as an important way to understand the kinetics of networks involving proofreading or similar branching structures. Moreover, any properties that involve only the ratio of stationary fluxes, such as error and cost studied here, are fully characterized with the knowledge of energy barriers, which are, in turn, fully captured by the partition ratio of fluxes without knowing all the reaction rates.

The significance of transition state energy is further elucidated in the MM-with-proofreading scheme. It is shown that while the energy barriers ($\epsilon^{\dagger}_{\lambda,R/W}$) affect error and cost, the difference of energy barriers between the correct and incorrect networks ($\Delta\epsilon^{\dagger}_{\lambda}$) fully determines the fundamental error–cost bound. More precisely, the energy barrier difference corresponds to the free energy difference between cognate and non-cognate substrates interacting with the enzyme in the same conformational state, which would be invariant under perturbations to the enzyme structure if a linear free energy relationship is assumed. The rate sampling is equivalent to perturbing the energy landscape without affecting the energy barrier difference, and the networks are optimized in the sense of tuning $\epsilon^{\dagger}$ with fixed $\Delta\epsilon^{\dagger}$. While the energy difference of discrete states is well characterized, for example, by the ratio of association constants, it is more difficult to determine the difference of energy barriers both experimentally and computationally. A system-specific molecular dynamic analysis of the transition state configuration might be useful to account for the barrier difference of $\Delta\epsilon^{\dagger}$,

which is the key to understanding how a specific biological discrimination process is kinetically controlled. Importantly, although the expression of the error–dissipation bound is system-specific, the theory and the kinetic control picture are general and by no means limited to the models studied here.

3.2. Constraints and strategies in real proofreading systems

The error–cost bound obtained in this work has several implications. First, although it is known that the minimum error always corresponds to infinite dissipation, the bound provides the complete quantitative description of how fast dissipation must increase and eventually diverge as error is decreased. It also helps to explain why several biological systems capable of achieving very low error maintain a relatively higher error instead [8,9,22]. Second, the multi-stage proofreading schemes reveal two approaches of reducing the cost at a given error: increasing the discrimination capacity of each proofreading pathway (f) or the number of proofreading pathways (n). In biological systems, however, the values of f and n are upper-bounded by various constraints. f is constrained by the difference in transition state energies, and n is limited since introducing new proofreading pathways requires the enzyme to have either additional conformational states or dedicated domains for proofreading, such as the editing site in aminoacyl-tRNA synthetases [34,48]. Depending on the biochemical structure as well as the functional purpose of the enzyme, one of the two constraints might be predominantly challenging to circumvent, resulting in the enzyme preferentially adopting the alternative strategy to reduce the energy cost of proofreading. However, the analysis in the multi-stage DBD scheme demonstrates that increasing n leads to a diminishing benefit of cost reduction compared to increasing f. This suggests that proofreading with fewer pathways and larger discrimination factors is favourable to proofreading with numerous pathways and small discrimination factors, potentially accounting for the rarity of multi-stage proofreading in nature. The method is also applied to models with multiple intermediate states, demonstrating that these states do not change the form of the bound.

The general applicability of our theoretical framework is demonstrated in three real biological proofreading networks. Surprisingly, the three systems seem to operate in different regimes. The DNA polymerase resides remarkably close to the error–dissipation bound, demonstrating high energy efficiency in DNA replication. By contrast, the ribosome is unable to optimize its energy dissipation, possibly as a consequence of maximizing speed. IleRS operates relatively close to the error–dissipation bound, but further optimization also seems to be prohibited by speed requirements. Therefore, although speed is in theory decoupled from the error–dissipation trade-off, it still plays an important role in the evolutionary trade-offs among characteristic properties due to realistic limitations to which biochemical reactions can be accelerated. The generalization of our formalism in these complex models allows identification of key states or mechanisms, which will be important to characterize experimentally. The theoretical optimal scheme requires the binding and unbinding reactions to be much faster than the subsequent reaction. In reality, however, such time-scale separation is not always possible since the binding/unbinding rates are upper-bounded by processes such as diffusion and substrate recognition, and the rate of the subsequent reaction is lower-bounded by the minimum overall reaction speed. Future studies generalizing the theoretical framework to include speed should take into consideration how these restrictions on rate constants constrain the free energy landscape and thereby affect the optimal error–cost bound.

Finally, our work provides a general framework of analysing the error–dissipation trade-off in biochemical reaction networks capable of achieving high fidelity with non-equilibrium proofreading. Given the importance of partition ratios, the error–cost bound could be determined as soon as a few key discrimination factors are measured. Further insights could be revealed by subjecting the energy barrier differences, which exert the key kinetic control on both error and dissipation, to a more detailed and specific molecular dynamics or experimental investigation. It would also be important to see the implication of the error–cost bound for other biological systems involving proofreading.

Data accessibility. All related data and derivations are provided in electronic supplementary material [49].

Authors' contributions. Q.Y.: conceptualization, formal analysis, investigation, methodology, visualization, writing–original draft, writing–review and editing; A.B.K.: conceptualization, formal analysis, funding acquisition, investigation, methodology, project administration, supervision, writing–original draft, writing–review and editing; O.A.I.: conceptualization, formal analysis, funding acquisition, investigation, methodology, project administration, supervision, writing–original draft, writing–review and editing. All authors gave final approval for publication and agreed to be held accountable for the work performed therein.

Competing interests. We declare we have no competing interests.

Funding. This work was supported by Welch Foundation grant no. C-1995 (to O.A.I.) and Center for Theoretical Biological Physics National Science Foundation (NSF) grant no. PHY-2019745. A.B.K. also acknowledges support from the Welch Foundation grant no. C-1559 and from NSF grant nos CHE-1664218 and MCB-1941106.

Acknowledgements. The authors thank D. Thirumalai, J. Gunawardena, F. Wong, U. Cetiner and K. Banerjee for valuable comments on the manuscript.

References

1. Kunkel TA, Bebenek K. 2000 DNA replication fidelity. *Annu. Rev. Biochem.* **69**, 497–529. (doi:10.1146/annurev.biochem.69.1.497)
2. Sydow JF, Cramer P. 2009 RNA polymerase fidelity and transcriptional proofreading. *Curr. Opin. Struct. Biol.* **19**, 732–739. (doi:10.1016/j.sbi.2009.10.009)
3. Rodnina MV, Wintermeyer W. 2001 Fidelity of aminoacyl-tRNA selection on the ribosome: kinetic and structural mechanisms. *Annu. Rev. Biochem.* **70**, 415–435. (doi:10.1146/annurev.biochem.70.1.415)
4. Zaher HS, Green R. 2009 Fidelity at the molecular level: lessons from protein synthesis. *Cell* **136**, 746–762. (doi:10.1016/j.cell.2009.01.036)

5. Hopfield JJ. 1974 Kinetic proofreading: a new mechanism for reducing errors in biosynthetic processes requiring high specificity. *Proc. Natl Acad. Sci. USA* **71**, 4135–4139. (doi:10.1073/pnas.71.10.4135)
6. Ninio J. 1975 Kinetic amplification of enzyme discrimination. *Biochimie* **57**, 587–595. (doi:10.1016/S0300-9084(75)80139-8)
7. Bennett CH. 1979 Dissipation-error tradeoff in proofreading. *Biosystems* **11**, 85–91. (doi:10.1016/0303-2647(79)90003-0)
8. Banerjee K, Kolomeisky AB, Igoshin OA. 2017 Elucidating interplay of speed and accuracy in biological error correction. *Proc. Natl Acad. Sci. USA* **114**, 5183–5188. (doi:10.1073/pnas.1614838114)
9. Mallory JD, Kolomeisky AB, Igoshin OA. 2019 Trade-offs between error, speed, noise, and energy dissipation in biological processes with proofreading. *J. Phys. Chem. B* **123**, 4718–4725. (doi:10.1021/acs.jpcb.9b03757)
10. Wong I, Patel SS, Johnson KA. 1991 An induced-fit kinetic mechanism for DNA replication fidelity: direct measurement by single-turnover kinetics. *Biochemistry* **30**, 526–537. (doi:10.1021/bi00216a030)
11. Gromadski KB, Rodnina MV. 2004 Kinetic determinants of high-fidelity tRNA discrimination on the ribosome. *Mol. Cell* **13**, 191–200. (doi:10.1016/S1097-2765(04)00005-X)
12. Savageau MA, Freter RR. 1979 Energy cost of proofreading to increase fidelity of transfer ribonucleic acid aminoacylation. *Biochemistry* **18**, 3486–3493. (doi:10.1021/bi00583a008)
13. Freter RR, Savageau MA. 1980 Proofreading systems of multiple stages for improved accuracy of biological discrimination. *J. Theor. Biol.* **85**, 99–123. (doi:10.1016/0022-5193(80)90284-2)
14. Savageau MA, Lapointe DS. 1981 Optimization of kinetic proofreading: a general method for derivation of the constraint relations and an exploration of a specific case. *J. Theor. Biol.* **93**, 157–177. (doi:10.1016/0022-5193(81)90062-X)
15. Ehrenberg M, Blomberg C. 1980 Thermodynamic constraints on kinetic proofreading in biosynthetic pathways. *Biophys. J.* **31**, 333–358. (doi:10.1016/S0006-3495(80)85063-6)
16. Blomberg C, Ehrenberg M. 1981 Energy considerations for kinetic proofreading in biosynthesis. *J. Theor. Biol.* **88**, 631–670. (doi:10.1016/0022-5193(81)90242-3)
17. Murugan A, Huse DA, Leibler S. 2012 Speed, dissipation, and error in kinetic proofreading. *Proc. Natl Acad. Sci. USA* **109**, 12 034–12 039. (doi:10.1073/pnas.1119911109)
18. Murugan A, Huse DA, Leibler S. 2014 Discriminatory proofreading regimes in nonequilibrium systems. *Phys. Rev. X* **4**, 021016. (doi:10.1103/PhysRevX.4.021016)
19. Wong F, Amir A, Gunawardena J. 2018 Energy-speed-accuracy relation in complex networks for biological discrimination. *Phys. Rev. E* **98**, 012420. (doi:10.1103/PhysRevE.98.012420)
20. Sartori P, Pigolotti S. 2013 Kinetic versus energetic discrimination in biological copying. *Phys. Rev. Lett.* **110**, 188101. (doi:10.1103/PhysRevLett.110.188101)
21. Sartori P, Pigolotti S. 2015 Thermodynamics of error correction. *Phys. Rev. X* **5**, 041039. (doi:10.1103/PhysRevX.5.041039)
22. Yu Q, Mallory JD, Kolomeisky AB, Ling J, Igoshin OA. 2020 Trade-offs between speed, accuracy, and dissipation in $tRNA^{Ile}$ aminoacylation. *J. Phys. Chem. Lett.* **11**, 4001–4007. (doi:10.1021/acs.jpclett.0c01073)
23. Mallory JD, Kolomeisky AB, Igoshin OA. 2020 Kinetic control of stationary flux ratios for a wide range of biochemical processes. *Proc. Natl Acad. Sci. USA* **117**, 8884–8889. (doi:10.1073/pnas.1920873117)
24. Mallory JD, Igoshin OA, Kolomeisky AB. 2020 Do we understand the mechanisms used by biological systems to correct their errors? *J. Phys. Chem. B* **124**, 9289–9296. (doi:10.1021/acs.jpcb.0c06180)
25. Hartich D, Barato AC, Seifert U. 2015 Nonequilibrium sensing and its analogy to kinetic proofreading. *New J. Phys.* **17**, 055026. (doi:10.1088/1367-2630/17/5/055026)
26. Galstyan V, Husain K, Xiao F, Murugan A, Phillips R. 2020 Proofreading through spatial gradients. *Elife* **9**, 771. (doi:10.7554/eLife.60415)
27. Mallory JD, Mallory XF, Kolomeisky AB, Igoshin OA. 2021 Theoretical analysis reveals the cost and benefit of proofreading in coronavirus genome replication. *J. Phys. Chem. Lett.* **12**, 2691–2698. (doi:10.1021/acs.jpclett.1c00190)
28. Shoval O, Sheftel H, Shinar G, Hart Y, Ramote O, Mayo A, Dekel E, Kavanagh K, Alon U. 2012 Evolutionary trade-offs, pareto optimality, and the geometry of phenotype space. *Science* **336**, 1157–1160. (doi:10.1126/science.1217405)
29. Piñeros WD, Tlusty T. 2020 Kinetic proofreading and the limits of thermodynamic uncertainty. *Phys. Rev. E* **101**, 022415. (doi:10.1103/PhysRevE.101.022415)
30. Johnson KA. 1993 Conformational coupling in DNA polymerase fidelity. *Annu. Rev. Biochem.* **62**, 685–713. (doi:10.1146/annurev.bi.62.070193.003345)
31. Estrada J, Wong F, DePace A, Gunawardena J. 2016 Information integration and energy expenditure in gene regulation. *Cell* **166**, 234–244. (doi:10.1016/j.cell.2016.06.012)
32. Hill TL. 1977 *Free energy transduction in biology*. New York, NY: Academic Press.
33. Qian H. 2006 Open-system nonequilibrium steady state: statistical thermodynamics, fluctuations, and chemical oscillations. *J. Phys. Chem. B* **110**, 15 063–15 074. (doi:10.1021/jp061858z)
34. Ling J, Reynolds N, Ibba M. 2009 Aminoacyl-tRNA synthesis and translational quality control. *Annu. Rev. Microbiol.* **63**, 61–78. (doi:10.1146/annurev.micro.091208.073210)
35. Cvetesic N, Perona JJ, Gruic-Sovulj I. 2012 Kinetic partitioning between synthetic and editing pathways in class I aminoacyl-tRNA synthetases occurs at both pre-transfer and post-transfer hydrolytic steps. *J. Biol. Chem.* **287**, 25 381–25 394. (doi:10.1074/jbc.M112.372151)
36. Dulic M, Perona JJ, Gruic-Sovulj I. 2014 Determinants for tRNA-dependent pretransfer editing in the synthetic site of isoleucyl-tRNA synthetase. *Biochemistry* **53**, 6189–6198. (doi:10.1021/bi5007699)
37. Cvetesic N, Bilus M, Gruic-Sovulj I. 2015 The tRNA A76 hydroxyl groups control partitioning of the tRNA-dependent pre- and post-transfer editing pathways in class I tRNA synthetase. *J. Biol. Chem.* **290**, 13 981–13 991. (doi:10.1074/jbc.M115.648568)
38. McKeithan TW. 1995 Kinetic proofreading in T-cell receptor signal transduction. *Proc. Natl Acad. Sci. USA* **92**, 5042–5046. (doi:10.1073/pnas.92.11.5042)
39. Kirsch JF. 1972 Linear free energy relationships in enzymology. In Advances in linear free energy relationships (eds NB Chapman, J Shorter), pp. 369–400. Boston, MA: Springer. (doi:10.1007/978-1-4615-8660-9_8).
40. Hammett LP. 1970 *Physical organic chemistry*. New York, NY: McGraw-Hill.
41. Çetiner U, Gunawardena J. 2020 Reformulating non-equilibrium steady-states and generalised Hopfield discrimination. (https://arxiv.org/abs/2011.14994)
42. Laidler KJ. 1987 *Chemical kinetics*. Englewood Cliffs, NJ: Prentice Hall.
43. Zaher HS, Green R. 2010 Hyperaccurate and error-prone ribosomes exploit distinct mechanisms during tRNA selection. *Mol. Cell* **39**, 110–120. (doi:10.1016/j.molcel.2010.06.009)
44. Wohlgemuth I, Pohl C, Mittelstaet J, Konevega AL, Rodnina MV. 2011 Evolutionary optimization of speed and accuracy of decoding on the ribosome. *Phil. Trans. R. Soc. B* **366**, 2979–2986. (doi:10.1098/rstb.2011.0138)
45. Belliveau NM, Chure G, Hueschen CL, Garcia HG, Kondev J, Fisher DS, Theriot JA, Phillips R. 2021 Fundamental limits on the rate of bacterial growth and their influence on proteomic composition. *Cell Syst.* **12**, 924–944.e2. (doi:10.1016/j.cels.2021.06.002)
46. Klumpp S, Scott M, Pedersen S, Hwa T. 2013 Molecular crowding limits translation and cell growth. *Proc. Natl Acad. Sci. USA* **110**, 16 754–16 759. (doi:10.1073/pnas.1310377110)
47. Bullwinkle TJ, Ibba M. 2014 Emergence and evolution. In Aminoacyl-tRNA synthetases in biology and medicine (ed. S Kim), pp. 43–87. Dordrecht, The Netherlands: Springer. (doi:10.1007/128_2013_423).
48. Nureki O *et al.* 1998 Enzyme structure with two catalytic sites for double-sieve selection of substrate. *Science* **280**, 578–582. (doi:10.1126/science.280.5363.578)
49. Yu Q, Kolomeisky AB, Igoshin OA. 2022 The energy cost and optimal design of networks for biological discrimination. Figshare.